✓

(12) LEVEL III

AD-E430 187

MEMORANDUM REPORT ARBRL-MR-02891

AD A0 66121

MUZZLE-BLAST-INDUCED TRAJECTORY PERTURBATION OF NONCONICAL AND CONICAL BOATTAIL PROJECTILES

DDC FILE COPY

Kevin S. Fansler
Edward M. Schmidt

January 1979

US ARMY ARMAMENT RESEARCH AND DEVELOPMENT COMMAND
BALLISTIC RESEARCH LABORATORY
ABERDEEN PROVING GROUND, MARYLAND

UNCLASSIFIED
SECURITY CLASSIFICATION OF THIS PAGE (When Data Entered)

REPORT DOCUMENTATION PAGE

READ INSTRUCTIONS BEFORE COMPLETING FORM

1. REPORT NUMBER: MEMORANDUM REPORT ARBRL-MR-02891
2. GOVT ACCESSION NO.:
3. RECIPIENT'S CATALOG NUMBER:

4. TITLE (and Subtitle): MUZZLE-BLAST-INDUCED TRAJECTORY PERTURBATION OF NONCONICAL AND CONICAL BOATTAIL PROJECTILES

5. TYPE OF REPORT & PERIOD COVERED: Final rept.

6. PERFORMING ORG. REPORT NUMBER:

7. AUTHOR(s): Kevin S. Fansler [redacted] Edward M. Schmidt

8. CONTRACT OR GRANT NUMBER(s):

9. PERFORMING ORGANIZATION NAME AND ADDRESS:
US Army Ballistic Research Laboratory
(ATTN: DRDAR-BLL)
Aberdeen Proving Ground, MD 21005

10. PROGRAM ELEMENT, PROJECT, TASK AREA & WORK UNIT NUMBERS: RDT&E 1L162618AH80

11. CONTROLLING OFFICE NAME AND ADDRESS:
US Army Armament Research & Development Command
US Army Ballistic Research Laboratory
(ATTN: DRDAR-BL)
Aberdeen Proving Ground, MD 21005

12. REPORT DATE: JAN [redacted]79

13. NUMBER OF PAGES: 29

14. MONITORING AGENCY NAME & ADDRESS (if different from Controlling Office):

15. SECURITY CLASS. (of this report): UNCLASSIFIED

15a. DECLASSIFICATION/DOWNGRADING SCHEDULE

16. DISTRIBUTION STATEMENT (of this Report)

Approved for public release; distribution unlimited.

AD-E

17. DISTRIBUTION STATEMENT (of the abstract entered in Block 20, if different from Report)

18. SUPPLEMENTARY NOTES

19. KEY WORDS (Continue on reverse side if necessary and identify by block number)

Spin-stabilized Projectiles
Transitional Ballistics
Free-flight Ballistics
Projectile Accuracy

20. ABSTRACT (Continue on reverse side if necessary and identify by block number)

Muzzle-blast loadings on spin-stabilized projectiles are analyzed and used to compute resultant trajectory deviations. Both conical and nonconical boattail rounds are treated. Approximations are made that permit the expression for the force on the projectile to be integrated; the resulting equation is used to develop a universal momentum transfer function that can be directly related to projectile jump. Although nonconical boattail configurations are more sensitive to muzzle blast than conical designs, the computed trajectory deviation in either case is small compared to the total measured dispersion of typical systems.

DD FORM 1 JAN 73 1473 EDITION OF 1 NOV 65 IS OBSOLETE

UNCLASSIFIED
SECURITY CLASSIFICATION OF THIS PAGE (When Data Entered)

393 471

TABLE OF CONTENTS

LIST OF ILLUSTRATIONS

1. INTRODUCTION

On the modern battlefield, weapon systems must shoot projectiles with a high degree of precision to lessen the chances of enemy return fire. Ideally, the weapon designer should be capable of quantifying the sources of dispersion in order to meet imposed precision standards. One source of perturbation to the desired trajectory is the gasdynamic force experienced in the weapon muzzle blast. For fin-stabilized projectiles, dispersion caused by the blast environment has been investigated [1,2]; however, treatment of spin-stabilized projectiles has been largely neglected. With the introduction of novel boattail designs[3], there is also interest in comparing the sensitivity to muzzle blast of the nonconical boattail configurations with the sensitivity of the conical boattail configurations.

The present paper examines the influence of muzzle-blast loadings upon the trajectory of spin-stabilized rounds. With both conical and nonconical boattail configurations, the analytical approach is similar to that used previously for fin-stabilized projectiles: namely, the most significant gasdynamic loadings are assumed to occur within the quasi-steady, supersonic core of the propellant gas jet. Pressure distributions on the projectiles are estimated utilizing steady-state flow theory and experiments. This procedure is not locally exact; however, it produces a reasonable estimate of the overall muzzle-blast-induced impulse. Transverse angular and linear momentums imparted by the blast are calculated for triangular, square and conical boattails and used to determine the contribution to the dispersion of 155mm, M549 type projectiles.

---

1. *E. M. Schmidt, K. S. Fansler, and D. D. Shear, "Trajectory Perturbations of Fin-Stabilized Projectiles Due to Muzzle Blast," Journal of Spacecraft and Rockets, Vol. 14, No. 6, June 1977, pp. 339-344.*

2. *K. S. Fansler, and E. M. Schmidt, "Trajectory Perturbations of Asymmetric Fin-Stabilized Projectiles Caused by Muzzle Blast," Journal of Spacecraft and Rockets, Vol. 15, No. 1, January-February 1978, pp. 62-64.*

3. *A. S. Platou, "An Improved Projectile Boattail," BRL MR 2395, US Army Ballistic Research Laboratories, Aberdeen Proving Ground, Maryland, July 1974. AD 785520.*

II. ANALYSIS OF GASDYNAMIC LOADS

Two distinct regions are considered. The first region for which a model is developed covers the flow following exit of the rotating/obturating band from the gun tube. When this band passes the muzzle, the gas seal is released, but the boattail is still within the tube and the forward portion of the projectile is immersed in the expanding propellant gases. The existence of asymmetry in this flow field due to projectile angle of attack results in transverse loads. For conical boattail rounds, these loads alter the transverse momentum; however, due to the cylindrical 'wheelbase' characteristic of non-conical boattail designs[3], momentum exchange occurs only when the non-planar surfaces are not contacting the bore. The second region of interest commences as the projectile base clears the muzzle and terminates as the base passes through the Mach disc of the propellant gas jet.

In both regions, the analysis seeks an upper-bound estimate of the propellant gas loadings. This approach is supported by previous upper-bound estimates[1,2] showing that muzzle-blast- induced dispersion of fin-stabilized projectiles is a negligible component of the total measured dispersion levels. Thus, it was not worthwhile to seek more accurate, but lower magnitude, estimates.

A. Region 1: Projectile base still within the bore

A schematic of the flow field is shown in Figure 1. For convenience, the flow behind the projectile is assumed to be sonic (occurs for $V_p \cong 700$ m/s). At separation of the obturating band, the propellant gases are released to expand into the atmosphere, generating the characteristic muzzle-blast wave. Due to the presence of the projectile, this free expansion is constrained and if the projectile is at an angle of attack, α_1, relative to the bore-line, the propellant gases will be deflected. Assuming that the projectile acts somewhat like a plug nozzle and that all of the flow is deflected through the angle α_1 at the sonic line, the resultant transverse lift force on the projectile can be simply estimated from momentum considerations:

$$L_1 = (p^* + \rho^* V^{*2}) A_u \alpha_1 \tag{1}$$

where A_u is the area of the muzzle that is unplugged (a function of boattail geometry), p^* is the pressure at the muzzle, ρ^* is the gas density at the muzzle and V^* is the gas velocity at the muzzle.

Equation (1) is an estimate for a stationary projectile. It may be corrected to account for projectile velocity. Consider a coordinate system moving with the projectile. The velocity of the fluid in this system is given as V_r. If the fluid near the projectile is deflected

to flow parallel to the projectile surface, the transformation between the stationary and moving coordinates is

$$V_r \exp (i\alpha_1) = V \exp (i\underline{\alpha}) - V_p \quad (2)$$

where $\underline{\alpha}$ is the turning angle for the fluid in the gun-tube coordinate system, V is the local velocity and V_p is the projectile velocity. We obtain:

$$\underline{\alpha} = (1 - V_p/V)\ \alpha_1 \quad (3)$$

The largest value for $\underline{\alpha}$ corresponds to the Mach number of the fluid approaching infinity. For $V_p = V^*$, the limiting value of V is 3 V_p and thus,

$$\underline{\alpha} = 2\alpha_1/3 \quad (4)$$

Thus to correct the lift force for projectile motion, we replace α_1 by $2\alpha_1/3$ in Equation (1). Using the isentropic flow relations, we obtain

$$L_1 = \frac{2}{3}(\gamma+1)\ p^*\ A_u\alpha_1 \quad (5)$$

The transverse momentum transferred to the projectile during the time between obturator separation and base emergence from the muzzle is the integral of the lift force over the time of passage. Transforming the variable of integration from time to distance, $t = (\underline{X}/D)\ (D/V_p)$, allows the momentum integral to be written:

$$P_1 = \frac{2}{3}(\gamma+1)\quad (D/V_p)p^*\alpha_1 \int A_u d(\underline{X}/D) \quad (6)$$

where $\underline{X}$ is the distance traveled since unplugging started and D is the bore diameter of the gun tube.

Nonconical Boattails.

The value of P_1 depends upon the boattail geometry because of the appearance of the vent area term, A_u, under the integral sign. This expression is addressed in detail in Appendix A where it is found for nonconical boattails that

$$P_1 = (16n/45)(\gamma+1)(p^*D^3/V_p)\theta^{3/2}\alpha_1(\underline{X}/D)^{5/2} \quad (7)$$

where n is number of plane boattail surfaces and θ is the boattail angle. The total amount of momentum transferred to the projectile by the venting flow is obtained by evaluating this expression at the maximum travel of the round, i.e., when the projectile base is at

the muzzle exit plane. For nonconical boattails that terminate in a polygon shape:

$$P_{1t} = [\pi^5/(90n^4)](\gamma+1)[p^*D^3/(\theta V_p)]\alpha_1 \tag{8}$$

It is useful to define a nondimensional momentum transfer function, $\overline{P}$, similar to that developed in Reference 4,

$$\overline{P} \equiv P/[(D/V_p)(\gamma+1)p^*A_{eq}\alpha_1] \tag{9}$$

For nonconical boattail projectiles, the surfaces are treated as miniature airfoils. In Reference 4, it was shown that the equivalent lifting surface area for a multiple-finned missile is $A_{eq} = nA/2$ for the lift vector in the angle-of-attack plane. Since the nonconical designs have only one surface to the "airfoil", the following definition is used:

$$A_{eq} = nA/4. \tag{10}$$

where A is the area of each plane surface.

This definition permits the momentum transfer functions to be written (See Appendix A, Equations A9 and A11)

$$\overline{P}_1 = (128/15)(n/\pi)^3 \ (\theta \underline{X}/D)^{5/2} \tag{11}$$

and

$$\overline{P}_{1t} = (4\pi^2)/(15n^2) \tag{12}$$

<u>Conical Boattails.</u>

Using the same approach, the momentum transfer function for a conical boattail design is

$$P_1 = (\pi/3) \ (\gamma+1) \ (p^*D^3/V_p)\theta\alpha_1 \ (\underline{X}/D)^2 \tag{13}$$

and in nondimensional form, with $A_{eq} = \pi D^2/4$:

---

4. *K. S. Fansler and E. M. Schmidt, "The Influence of Muzzle Gasdynamics Upon the Trajectory of Fin-Stabilized Projectiles," BRL R 1793, U. S. Army Ballistic Research Laboratory, Aberdeen Proving Ground, MD, June 1975. AD B005379L.*

$$\bar{P}_1 = (40/3)(\underline{X}/D)^2 \quad (14)$$

B. Region 2: Projectile Base out of the gun tube

Nonconical Boattails.

There are no data available describing the aerodynamics of nonconical boattails in reverse flow. Since the three-dimensional nature of the muzzle flow makes direct computation difficult, the lift force on the boattail will be estimated using two-dimensional airfoil theory. This approximation neglects any effects of base bluntness due to truncation of the boattail; however, the side force on a bluff body is generally smaller than that on a slender body at an equal angle of attack. Therefore, the current approximation should produce an upper bound on the transverse force exerted on these nonconical surfaces by muzzle gas loadings. The value of $\bar{P}_2(\underline{X}/D)$ can be obtained directly from earlier results[1] using the definition of A_{eq} in Equation (10). The center of force is taken as the area centroid for the plane surfaces. This center of force value would be correct for two-dimensional supersonic airfoil theory but may be quite different from the possible actual results. Nevertheless, for this analysis, the approximation should be sufficient since the percent error between differing possible moment-arm values would be small.

Conical Boattails.

The transverse force on conical boattail projectiles is estimated using experimental data[5] acquired on blunt, flared sphere-cones at a variety of Mach numbers. These data were obtained using a sphere-cone where the ratio of the diameter of the cone at the sphere-cone junction to the base diameter was 0.8. The smallest cone half-angle of this set of data was 10°. For the purposes of the present analysis, it is desired to compare the muzzle blast sensitivity of a 7° nonconical boattail with the sensitivity of a similar half-angle cone. Thus, the data[5] are extrapolated to this angle, Figure 2. The center of force is taken to be halfway along the boattail length.

---

5. *A. D. Foster, "A Compilation of Longitudinal Aerodynamic Characteristics Including Pressure Information for Sharp and Blunt-nose Cones Having Flat and Modified Bases," Sandia Corporation Report No. SC-R-64-1311, January 1965.*

III. RESULTS AND DISCUSSION

The M549 projectile is used as a basis for the computations since flight data are available on this round with both the standard 7^o boattail and a triangular boattail. The properties of the projectiles are given in the tables below.

Table I: M549 Parameters Independent of Boattail

$$M_p = 43.0 \text{ kg}$$

$$D = 0.155\text{m}$$

$$V_p = 670\text{m/s}$$

$$p^* = 1.52 \times 10^7 \text{ Pa}$$

$$\gamma = 1.25$$

$$C_{M_\alpha} = 3.30$$

$$C_{L_\alpha} = 2.95$$

$$I_x = 0.13 \text{ kg-m}^2$$

Table II. M549 Parameters Dependent on Boattail

	Standard Conical	Triangular NCBT	Square NCBT
A_{eq} (m^2)	0.0189	0.028	0.016
θ(deg)	7	7	7
Δ(m)	0.295	0.293	0.340
ℓ(m)	0.097	0.347	0.195
I_y(kg-m^2)	1.93	1.71	1.71

Here Δ is the distance between the force acting on the planar surface and the center of gravity; ℓ is the length of the boattail.

The values of $\overline{P}$ through both the in-bore and exterior regions of interest are shown in Figures 3-5 for the three boattails considered.

The coordinate X is the location of the projectile center of pressure along the bore axis, with X = 0 corresponding to the muzzle. Since the momentum transfer function is cummulative, the asymptotic value of each curve is equal to the total momentum $\bar{P}_t$ transferred in the blast. From Equation (14), it is apparent that the $\bar{P}_{1t}$ for the conical boattail has an explicit dependence on ℓ/D and θ; however, for the nonconical boattails considered (those taken back to the intersection of planar surfaces), this is not the case. $\bar{P}_{1t}$ and $\bar{P}_t$ are independent of all boattail and projectile parameters, i.e., the curves are 'universally' applicable to any projectile with an n-sided nonconical boattail launched with the velocity of the exit-gas speed of sound.

The momentum functions are used to compute the transverse angular and linear velocities imparted to the projectiles in the blast region, using the approach of Reference 4. These velocities are input to the aerodynamic jump relations[6] for conical boattails, resulting in

$$\Theta/\alpha_1 = [1+(C_{L_\alpha}\Delta)/(C_{M_\alpha} D)]\ (\gamma+1)p^*A_{eq}[D/(M_pV_p^{\ 2})]\ \bar{P}_t \qquad (15)$$

For nonconical boattails, the working equation, using Equations (10) and (A12), is

$$\Theta/\alpha_1 = [\pi^3\ (\gamma+1)/24]\ [p^*D^3/(M_pV_p^{\ 2})]\ [1+(C_{L_\alpha}\Delta)/(C_{M_\alpha} D)][\bar{P}_t/n^2\theta)] \qquad (16)$$

An expression for the first maximum yaw may also be derived[6]:

$$|\xi_{max}|/\alpha_1 = [2(\gamma+1)\ A_{eq}\Delta D^2\ p^*\ \bar{P}_t/(I_yV_p^{\ 2})]/[(I_x\phi'_o/I_y)^2 - \pi\rho D^5C_{M_\alpha}/(2I_y)]^{\frac{1}{2}} \qquad (17)$$

For nonconical boattails, the working equation is, using Equations (A12) and (10),

$$|\xi_{max}|/\alpha_1 = [\ \pi^3\ (\gamma+1)/12]\ [\Delta D^4\ p^*\ \bar{P}_t/(I_yV_p^{\ 2}\ n^2\theta)]$$

$$\cdot [(I_x\phi'_o/I_y)^2 - \pi\rho D^5C_{M_\alpha}/(2I_y)]^{\frac{1}{2}} \qquad (18)$$

Here ϕ_o' is the initial spin in radians per caliber.

---

6. *C. H. Murphy, "Free Flight Motion of Symmetric Missiles," U.S. Army Ballistic Research Laboratories Report Number 1216, Aberdeen Proving Ground, Maryland, July 1963. AD 442757.*

The projectile parameters from Tables I and II with the above relations are used to determine the values in the following table:

Table III. Launch Dynamic Characteristics

	Standard Conical	Square NCBT	Triangular NCBT
$\overline{P}_t$	0.21	0.52	0.48
$\lvert\xi_{max}\rvert/\alpha_1$ (deg/deg)	0.167	0.37	0.57
Θ/α_1 (mil/deg)	0.051	0.11	0.18
$\lvert\xi_{max}\rvert$ (degs for 1σ with $\alpha_1 = 0.1^o$)	0.02	0.04	0.06

Comparing these results for Θ/α_1 with those obtained for fin-stabilized projectiles[1], we find that the values are similar.

Table III shows that the jump sensitivity of the nonconical boattail rounds is more than twice that of the standard conical boattail. However, the last row gives the contribution to the first maximum yaw of this muzzle-blast-induced jump. For a reasonable distribution of the in-bore yaw level ($1\sigma, \alpha_1 \cong 0.1^o$), the resultant contribution to the first maximum yaw is 0.06^o in the worst case. This value is judged negligible compared with the frequently observed first-maximum yaw values for the M549 of approximately 5^o. Since the first-maximum-yaw value is proportional to the aerodynamic jump, we may infer that muzzle blast contributes only a small amount to the total observed dispersion.

IV. SUMMARY AND CONCLUSIONS

A model is developed to determine the effect of muzzle gasdynamic loadings upon the trajectory of spin-stabilized projectiles for both conical and nonconical boattail configurations. The analysis consists of two parts. First, the passage of the boattail out of the gun following separation of the obturator is addressed. Second, the region exterior to the muzzle but prior to the projectile's passage through the Mach disc is modelled. The conical boattail aerodynamics are determined from experimental data acquired on sphere cones; two-dimensional airfoil theory is applied to approximate the loadings on nonconical boattails.

Expressions for the loadings are integrated to determine the momentum transferred to each of the M549 projectile configurations launched at a muzzle velocity of 670 m/s from a 155mm gun. The non-conical boattail configurations are found to be more than twice as

sensitive to blast as the conical design; however, in neither case is the contribution to dispersion due to muzzle gasdynamic loadings significant when compared to the total dispersion of the gun system.

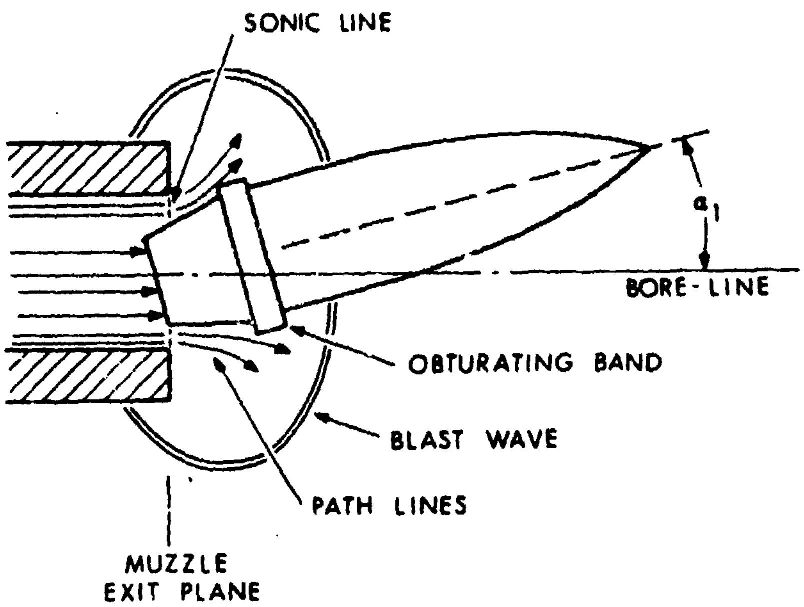

Figure 1. Flowfield schematic

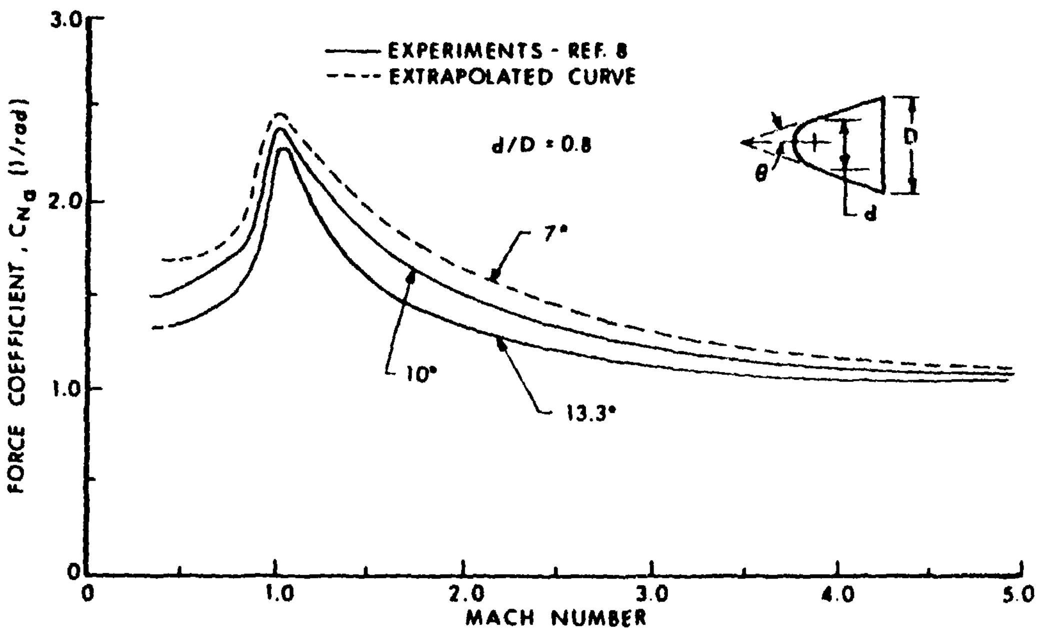

Figure 2. Experimental and extrapolated lift data for sphere-cones

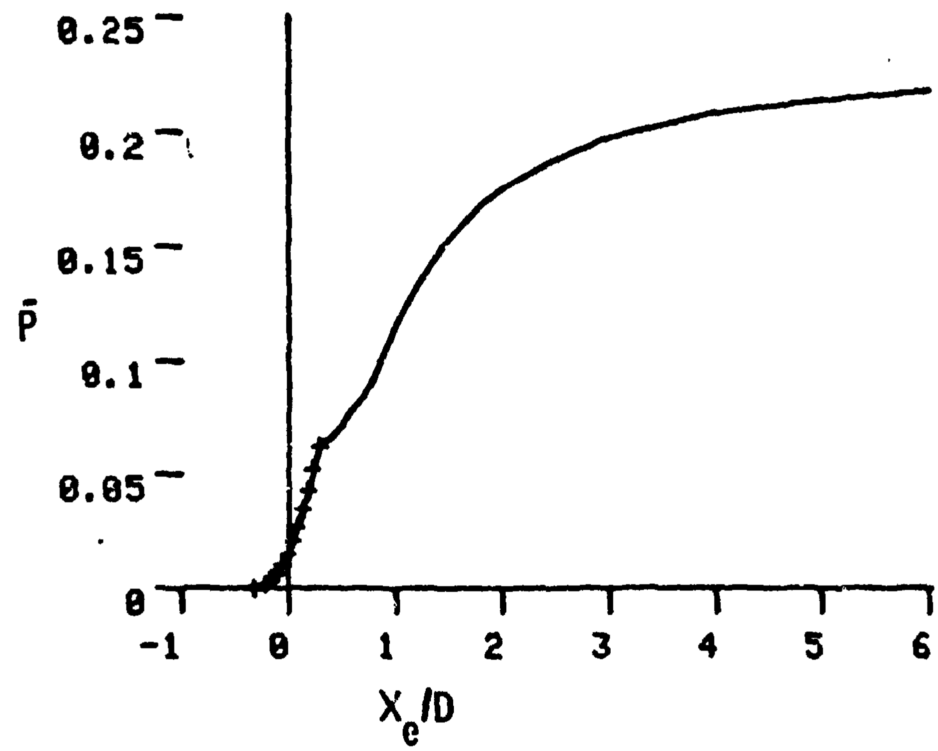

Figure 3. Momentum function for the conical 549 boattail

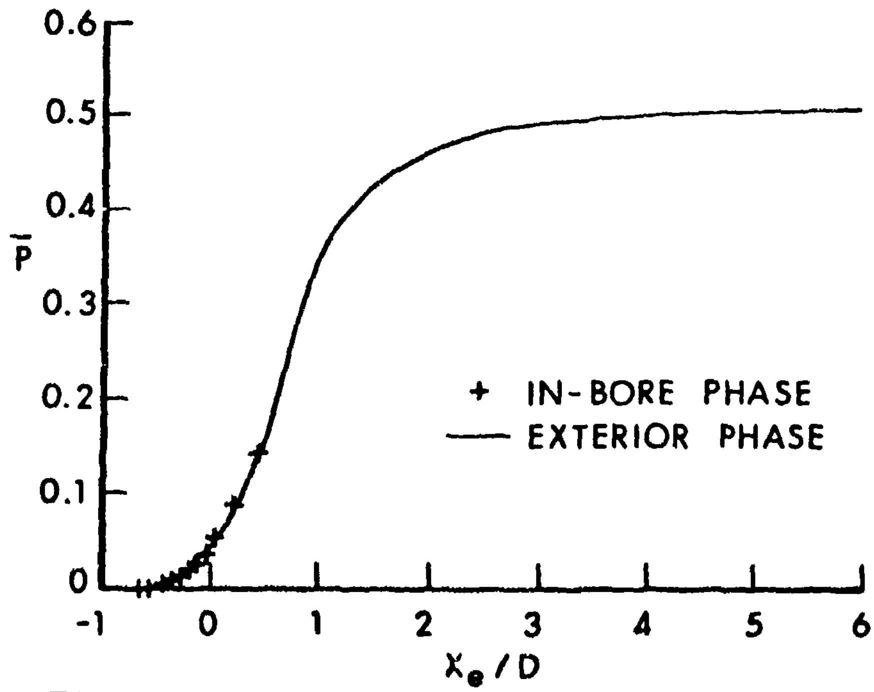

Figure 4. Momentum function for the square boattail

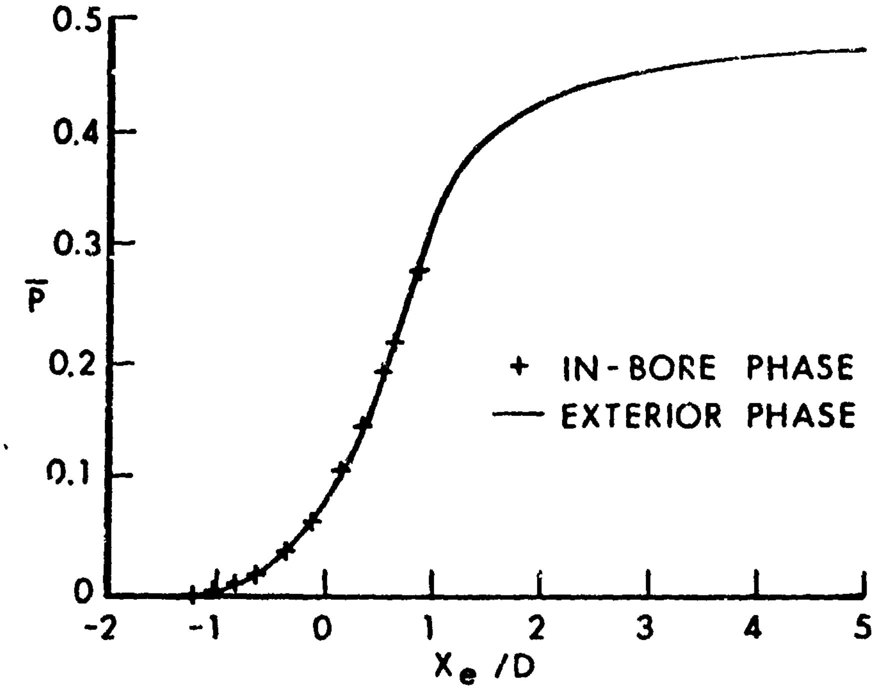

Figure 5. Momentum function for the triangular boattail

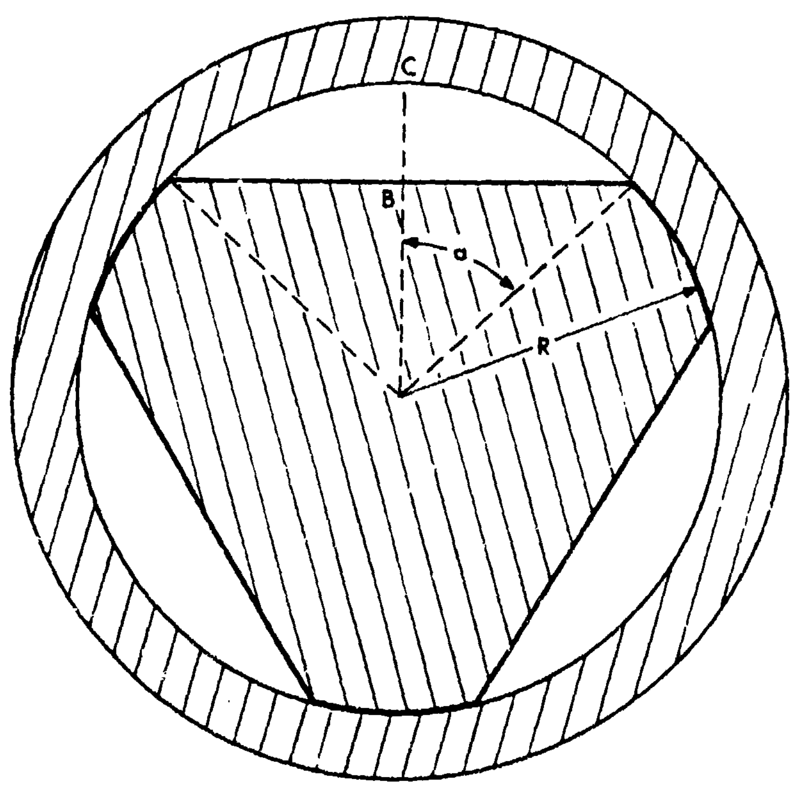

Figure 6. Cross-section of nonconical boattail in muzzle plane

REFERENCES

1. E. M. Schmidt, K. S. Fansler, and D. D. Shear, "Trajectory Perturbations of Fin-Stabilized Projectiles Due to Muzzle Blast," Journal of Spacecraft and Rockets, Vol. 14, No. 6, June 1977, pp. 339-344.

2. K. S. Fansler, and E. M. Schmidt, "Trajectory Perturbations of Asymmetric Fin-Stabilized Projectiles Caused by Muzzle Blast," Journal of Spacecraft and Rockets, Vol. 15, No. 1, January-February 1978, pp. 62-64.

3. A. S. Platou, "An Improved Projectile Boattail," BRL MR 2395, US Army Ballistic Research Laboratories, Aberdeen Proving Ground, Maryland, July 1974. AD 785520.

4. K. S. Fansler and E. M. Schmidt, "The Influence of Muzzle Gasdynamics Upon the Trajectory of Fin-Stabilized Projectiles," BRL R 1793, U.S. Army Ballistic Research Laboratories, Aberdeen Proving Ground, MD, June 1975. AD B005379L.

5. A. D. Foster, "A Compilation of Longitudinal Aerodynamic Characteristics Including Pressure Information for Sharp and Blunt-nose Cones Having Flat and Modified Bases," Sandia Corporation Report No. SC-R-64-1311, January 1965.

6. C. H. Murphy, "Free Flight Motion of Symmetric Missiles," U.S. Army Ballistic Research Laboratories Report Number 1216, Aberdeen Proving Ground, Maryland, July 1963. AD 442757.

APPENDIX A. EXPRESSION FOR TRANSVERSE MOMENTUM

In order to evaluate the integral in Equation (6), it is desirable to obtain closed-form expressions for A_u.

A. Nonconical Boattail

Figure 6 shows the cross section of a boattail in the muzzle plane. The bore radius is R and the area of the circular segment can be readily determined to be

$$A_{u_1} = R^2 \, (a - \sin 2a/2) \tag{A1}$$

The expression in brackets may be expanded in series yielding:

$$A_{u_1} = \frac{D^2}{6} \left(a^3 - \frac{a^5}{5} + \frac{2}{105} \; a^7 - \ldots .\right) \tag{A2}$$

In keeping with the upper bound approach, the series is truncated after the first term to give

$$A_{u_1} = D^2 a^3/6 \tag{A3}$$

The distance BC, Figure 6, is

$$\begin{aligned} BC &= R[1-\cos(a)] \\ &= \frac{R}{2} \left(a^2 - a^4/12 + \ldots\right) \end{aligned} \tag{A4}$$

However, BC is also related to the boattail angle and the length, $\underline{X}$, of the nonconical surfaces protruding beyond the muzzle plane.

$$BC = \underline{X} \tan\theta \tag{A5}$$

Assuming small θ and taking the first term in the series of Equation (A4) gives

$$a^2 = 4\theta \, \underline{X}/D \tag{A6}$$

which can be substituted into Equation (A3):

$$A_{u_1} = (4D^2/3) \;\; (\underline{X}/D)^{3/2} \theta^{3/2} \tag{A7}$$

For an n-sided boattail,

$$A_u = nA_{u_1} = (4nD^2/3)\,(\underline{X}/D)^{3/2} \theta^{3/2} \tag{A8}$$

This formulation for A_u may be substituted into Equation (6) and integrated to provide

$$P_1 = (\gamma+1)[16\ nD^3 p^* \alpha_1/45\ V_p]\ \theta^{3/2}\ (\underline{X}/D)^{5/2} \tag{A9}$$

If the boattail terminates where the planar surfaces intersect, then

$$a_m = \pi/n. \tag{A10}$$

This permits the evaluation of the total momentum transferred in-bore:

$$P_{1t} = (\pi^5/90\ n^4)(\gamma+1)(p^* D^3/\theta V_p)\ \alpha_1 \tag{A11}$$

This type of boattail has a surface area that can be readily computed. Since the surface is an ellipse formed by intersecting the cylindrical body with a plane at angle θ to the axis,

$$A = A_{u_1}/\theta \quad \text{(evaluated at the muzzle station)}$$

$$= D^2\ (\pi/n)^3/(6\theta) \tag{A12}$$

B. <u>Conical Boattail</u>

The unplugged area is

$$A_u = \pi(R^2 - r^2) \tag{A13}$$

where r is the diameter of the section of the boattail passing the muzzle plane. Since $R - r = \underline{X}\ \tan\theta \cong \underline{X}\ \theta$,

$$A_u = \pi\,(2R - \underline{X}\ \theta)\ \underline{X}\theta\quad , \tag{A14}$$

which may be substituted into Equation (6) to give

$$P_1 = (\pi/3)(\gamma+1)(p^* D^3/V_p)\ \theta\ (\underline{X}/D)^2\ \alpha_1 \tag{A15}$$

LIST OF SYMBOLS

a	= angle defined in Figure 6
A	= area of a plane surface of the nonconical boattail
A_{eq}	= the equivalent area of an airfoil in two-dimensional flow
A_u	= the area at the muzzle that is unplugged
C_{DR}	= projectile drag coefficient in muzzle blast
C_{L_α}	= slope of the lift coefficient curve for forward flight
C_{M_α}	= slope of the static moment coefficient curve in forward flight
D	= the diameter of the bore and projectile
I_x	= axial moment of inertia
I_y	= transverse moment of inertia
L	= the lift force on the projectile
L_1	= lift force on projectile in the first part of its transit
ℓ	= length of boattail
M_p	= projectile mass
n	= the number of plane surfaces possessed by the boattail
p	= pressure
P	= the momentum given the projectile
P_1	= momentum given the projectile during the first part of the projectile's transit
$\overline{P}$	= the value of P nondimensionalized according to Equation (10)
$\overline{P}_t$	= the total amount of $\overline{P}$ imparted by the muzzle blast

t	= time variable
V	= local velocity of gases
V_p	= velocity of projectile
V_r	= velocity of gases relative to a coordinate system located on the projectile
x	= position along the axis of the center of force for the projectile relative to the muzzle
$\underline{x}$	= distance traveled since unplugging started
y	= axis coordinate in the angle of attack plane that is perpendicular to the x-axis
α	= maximum angle between projectile and gun-tube axis--angle of attack
$\underline{\alpha}$	= angle determined by α and fluid flow velocity relative to the projectile
α_1	= angle of attack upon emergency from muzzle
α_o	= angle of attack upon emergency from muzzle blast
α'	= derivative of α with respect to distance in calibers
α'_o	= value of α' upon emergency from muzzle blast
γ	= ratio of specific heats
Δ	= distance from center of force to center of gravity for flight through muzzle-blast region
ξ	= complex angle of attack
ϕ	= roll angle of projectile
θ	= boattail angle
Θ	= aerodynamic jump
ρ	= local density of gases

DISTRIBUTION LIST

No. of Copies	Organization
12	Commander Defense Documentation ATTN: DDC-DDA Cameron Station Alexandria, VA 22314
1	Director Defense Nuclear Agency Washington, DC 20305
1	Commander US Army Materiel Development and Readiness Command ATTN: DRCDMD-ST, N. Klein 5001 Eisenhower Avenue Alexandria, VA 22333
1	Commander US Army Materiel Development and Readiness Command ATTN: DRCDL 5001 Eisenhower Avenue Alexandria, VA 22333
3	Commander US Army Aviation Research and Development Command ATTN: DRSAV-E DRCPM-AAH, M. Corgiatt Product Manager, AH-1, D. Brewer 12th and Spruce Streets St. Louis, MO 63166
1	Director US Army Air Mobility Research and Development Laboratory Ames Research Center Moffett Field, CA 94035
1	Commander US Army Electronics Research and Development Command Technical Support Activity ATTN: DELSD-L Fort Monmouth, NJ 07703

No. of Copies	Organization
1	Commander US Army Communications Rsch and Development Command ATTN: DRDCO-PPA-SA Fort Monmouth, NJ 07703
1	Commander US Army Jefferson Proving Ground ATTN: STEJP-TD-D Madison, IN 47250
3	Commander US Army Missile Research and Development Command ATTN: DRDMI-R DRDMI-RBL DRDMI-RDK Redston Arsenal, AL 35809
1	Commander US Army Missile Materiel Readiness Command ATTN: DRSMI-AOM Redstone Arsenal, AL 35809
1	Commander US Army Tank Automotive Rsch and Development Command ATTN: DRDTA-UL Warren, MI 48090
1	Commander US Army Mobility Equipment Research & Development Cmd ATTN: DRDME-WC Fort Belvoir, VA 22060
2	Commander US Army Armament Materiel Readiness Command ATTN: DRSAR-LEP-L, Tech Lib DRSAR-RDG, J. Blick Rock Island, IL 61299

DISTRIBUTION LIST

No. of Copies	Organization
5	Commander US Army Armament Research and Development Command ATTN: DRDAR-TSS (2 cys) DRDAR-TDS, Mr. Lindner DRDAR-LC-F, Mr. A.Loeb Mr. S. Friedman Dover, NJ 07801
4	Commander US Army Armament Research and Development Command ATTN: DRDAR-LCV, Mr.Barrieres Mr. R. Reisman DRDAR-SCN, Mr. Kahn PM, XM788/789, LTC Delany Dover, NJ 07801
5	Commander US Army Watervliet Arsenal ATTN: DRDAR-LCB-TL, Tech Lib, (2 cys) Mr. W. Dock Dr. G. Carofano Mr. P. Alto Watervliet, NY 12189
1	Commander US Army Materiels and Mechanics Research Center Watertown, MA 02172
1	Commander US Army Natick Research and Development Command ATTN: DRXRE, Dr. D. Sieling Natick, MA 01762
1	Director US Army TRADOC Systems Analysis Activity ATTN: ATAA-SL, Tech Lib White Sands Missile Range NM 88002
1	HQDA (DAMA-WSA, MAJ Fite) Washington, DC 20310
1	Commander US Army Research Center ATTN: CRD-AA-EH P. O. Box 12211 Research Triangle Park NC 27709
1	Director US Army BMD Advanced Technology Center P.O. Box 1500, West Station Huntsville, AL 35807
1	Commander US Army Ballistic Missile Defense Systems Command Huntsville, AL 35804
3	Commander Naval Air Systems Command ATTN: AIR-604 Washington, DC 20360
3	Commander Naval Ordnance Systems Command ATTN: ORD-9132 Washington, DC 20360
2	Commander and Director David W. Taylor Naval Ship Research & Development Ctr ATTN: Lib Div, Code 522 Aerodynamic Lab Bethesda, MD 20084
3	Commander Naval Surface Weapons Center ATTN: Code 6X Mr. F. H. Maille Dr. J. Yagla Dr. G. Moore Dahlgren, VA 22448

DISTRIBUTION LIST

No. of Copies	Organization
1	Commander Naval Surface Weapons Center ATTN: Code 730, Tech Lib Silver Spring, MD 20910
1	Commander Naval Weapons Center ATTN: Code 553, Tech Lib China Lake, CA 93555
1	Commander Naval Research Laboratory ATTN: Tech Info Div Washington, DC 20375
1	Commander Naval Ordnance Station ATTN: Code FS13A, P. Sewell Indian Head, MD 20640
1	AFRPL/LKCB, Dr. Horning Edwards AFB, CA 93523
2	AFATL (DLDL, D. C. Daniel; Tech Lib) Eglin AFB, FL 32542
1	AFWL/DEV Kirtland AFB, NM 87117
1	ASD/XRA (Stinfo) Wright-Patterson AFB, OH 45433
1	Director National Aeronautics and Space Administration George C. Marshall Space Flight Center ATTN: MS-I, Lib Huntsville, AL 35812
1	Director Jet Propulsion Laboratory ATTN: Tech Lib 2800 Oak Grove Drive Pasadena, CA 91103
1	Director National Aeronautics and Space Administration Langley Research Center ATTN: MS 185, Tech Lib Langley Station Hampton, VA 23365
1	Director NASA Scientific & Technical Information Facility ATTN: SAK/DL P. O. Box 8757 Baltimore/Washington International Airport, MD 21240
1	AAI Corporation ATTN: Dr. T. Stastny Cockeysville, MD 21030
1	Advanced Technology Labs ATTN: Dr. J. Erdos Merrick & Steward Avenues Westbury, NY 11590
1	Aerospace Corporation ATTN: Dr. T. Taylor P. O. Box 92957 Los Angeles, CA 90009
1	ARO, Inc. ATTN: Tech Lib Arnold AFS, TN 37389
1	ARO, Inc. Von Karman Gasdynamics Facility ATTN: Dr. J. Adams Arnold AFS, TN 37389
1	ARTEC Associates, Inc. ATTN: Dr. S. Gill 26046 Eden Landing Road Hayward, CA 94545

DISTRIBUTION LIST

No. of Copies	Organization
1	AVCO Systems Division ATTN: Dr. W. Reinecke 201 Lowell Street Wilmington, MA 01887
1	Battelle Columbus Laboratories ATTN: J. E. Backofen, Jr. 505 King Avenue Columbus, OH 43201
1	Technical Director Colt Firearms Corporation 150 Huyshore Avenue Hartford, CT 14061
2	General Electric Corporation Armaments Division ATTN: Mr. R. Whyte Mr. J. MacNeil Lakeside Avenue Burlington, VT 05401
1	Honeywell, Inc. ATTN: Mail Station MN 112190 (G. Stilley) 600 Second Street, North Hopkins, MN 55343
3	Hughes Helicopter Company Bldg. 2, MST22B ATTN: Mr. T. Edwards Mr. J. Johnson Mr. R. Forker Centinella & Teale Streets Culver City, CA 90230
1	Martin Marietta Aerospace ATTN: Mr. A. J. Culotta P. O. Box 5387 Orlando, FL 32805
1	Winchester-Western Division Olin Corporation New Haven, CT 06504

No. of Copies	Organization
1	Rockwell Int'l Science Center ATTN: Dr. Norman Malmuth P. O. Box 1085 1000 Oaks, CA 91360
1	Sandia Laboratories ATTN: Aerodynamics Dept Org 5620, R. Maydew Albuquerque, NM 87115
1	S&D Dynamics, Inc. ATTN: Dr. M. Soifer 755 New York Avenue Huntington, NY 11743
1	Guggenheim Aeronautical Lab California Institute of Tech ATTN: Tech Lib Pasadena, CA 91104
1	Franklin Institute ATTN: Tech Lib Race & 20th Streets Philadelphia, PA 19103
1	Director Applied Physics Laboratory The Johns Hopkins University Johns Hopkins Road Laurel, MD 20810
1	Massachusetts Institute of Tech Dept of Aeronautics and Astronautics ATTN: Tech Lib 77 Massachusetts Avenue Cambridge, MA 02139
1	Ohio State University Dept of Aeronautics and Astronautical Engineering ATTN: Tech Lib Columbus, OH 43210

DISTRIBUTION LIST

No. of Copies	Organization
2	Polytechnic Institute of New York Graduate Center ATTN: Tech Lib Dr. G. Moretti Route 110 Farmingdale, NY 11735
1	Director Forrestal Research Center Princeton University Princeton, NJ 08540
1	Forrestal Campus Library Princeton University ATTN: Dr. M. Summerfield P. O. Box 710 Princeton, NJ 08540
1	Southwest Research Institute ATTN: Mr. Peter S. Westine P. O. Drawer 28510 8500 Culebra Road San Antonio, TX 78228

Aberdeen Proving Ground

Dir, USAMSAA
ATTN: Dr. J. Sperrazza
DRXSY-MP, H. Cohen
Cdr, USA CSL/EA (Bldg. E3516)
ATTN: A. Flatau, SAREA-DE-W
Cdr, USATECOM
ATTN: DRSTE-SG-H